



Few-layer Bi₂Se₃-based passively Q-switched Pr:YLF visible lasers



Saiyu Luo^a, Xigun Yan^a, Bin Xu^a, Liangping Xiao^b, Huiying Xu^a, Zhiping Cai^{a,*}, Jian Weng^c

^a Department of Electronic Engineering, Xiamen University, Xiamen 361005, China

^b Department of Chemical & Biochemical Engineering, National Engineering Laboratory for Green Chemical Productions of Alcohols, Ethers and Esters, Xiamen University, Xiamen 361005, China

^c Department of Biomaterials, Xiamen University, Xiamen 361005, China

ARTICLE INFO

Keywords:

Diode-pumped
Passive Q-switching
Few-layer Bi₂Se₃
Visible

ABSTRACT

We report on diode-pumped Q-switched Pr:YLF lasers at deep red ~721 nm, red ~640 nm and orange ~(607 + 604) nm, using a few-layer Bi₂Se₃ saturable absorber. The narrowest pulse widths, maximum pulse energies and pulse peak powers have been achieved to be about (368 ns, 0.17 μJ, 0.46 W), (210 ns, 0.16 μJ, 0.73 W) and (263 ns, 0.19 μJ, 0.71 W), respectively for the three wavelengths. This work reveals that Bi₂Se₃ is a promising saturable absorber for visible solid-state lasers.

© 2017 Published by Elsevier B.V.

1. Introduction

Nanomaterials used as saturable absorber (SA) are of great interest and therefore have attracted a lot of attention during the past decade [1–5]. Efforts have been made to explore all these high-performance nanomaterials because of their excellent properties, such as ultra-broadband saturable absorption, low cost and easy fabrication.

At present, one of the important research topics for such nanomaterial SAs is to extend their operational wavelengths further towards MIR and visible spectral regions. For instance, recently, using black phosphorus [6], graphene [7] and MoS₂ [8] as SAs, Q-switched lasers have been successfully operated at ~2.8 μm and the shortest pulse width was reported to be 335 ns [8]. In terms of visible lasers, for example, in 2015, Zhang et al. [9] reported MoS₂-based visible Q-switched lasers at 605, 639 and 721 nm with pulse widths of 278 ns, 403 ns and 382 ns using Pr:GLF as gain medium. Using Au nanorods as saturable absorber, pulse widths of 237 ns, 152 ns and 318 ns respectively at the three wavelengths have also been achieved by researchers from the same group [10]. Meanwhile, Cr:YAG, as one of the mostly used conventional saturable absorbers, has also been used to generate visible pulsed lasers [11]. At present, compared to these novel nanomaterials saturable absorbers, Cr:YAG has advantage in generating Q-switched lasers with narrower pulse widths. However, bulk Cr:YAG has degraded the compactness of the laser system. Moreover, Cr:YAG does not possess ultra-broadband saturable absorption.

Recently, topological insulators (TIs) have also appeared to be potential as SAs, which exhibit large third-order nonlinear optical

response [12]. They also show ultra-broadband saturable absorption like graphene, but they exhibit much higher modulation depth than graphene [13]. On the one hand, the operational wavelength of TIs has also been extended to wider ranges like other nanomaterial SAs [12–17]. For instance, Q-switched 2.8-μm Er-ZBLAN fiber laser using Bi₂Te₃ was also reported with 1.3 μs pulse duration [17]. On the other hand, Bi₂Se₃, representative of the TIs, has been mostly studied [12–16]. For instance, Yu et al. [12] reported the first Bi₂Se₃-based Q-switched laser using Nd:GdVO₄ as gain medium and obtained 58.5 nJ single pulse energy. In 2015, Xu et al. [14] reported a Q-switched Nd:YLF laser at 1313 nm with a pulse width of 433 ns. Recently, using Bi₂Se₃ and Bi₂Te₃ as SAs, Wu et al. [15] in our group reported a Q-switched Pr-ZBLAN fiber laser at 635 nm with maximum output power of 5.1 mW, the shortest pulse width of 327 ns and pulse energy of 14.3 nJ, which has represented the first work of Q-switched lasers at visible using topological insulator as saturable absorber. Cheng et al. [16] demonstrated the first Bi₂Se₃-based solid-state visible laser at 604 nm using Pr:YLF crystal as gain medium. The achieved shortest pulse width was limited to 802 ns by the long laser cavity. Therefore, on the one hand, the present laser results concerning the Q-switched laser operation at visible need to be further upgraded, for example, in augmenting the average output power of the 635-nm red laser and in narrowing the pulse width of the 604-nm orange laser. On the other hand, the saturable absorption property of the topological insulator should be further explored towards broader wavelength range.

Motivated by the state of the art of topological insulator based visible laser, in this work, using few-layer TI Bi₂Se₃ as SA and Pr:YLF as gain

* Corresponding author.

E-mail address: zpcai@xmu.edu.cn (Z. Cai).

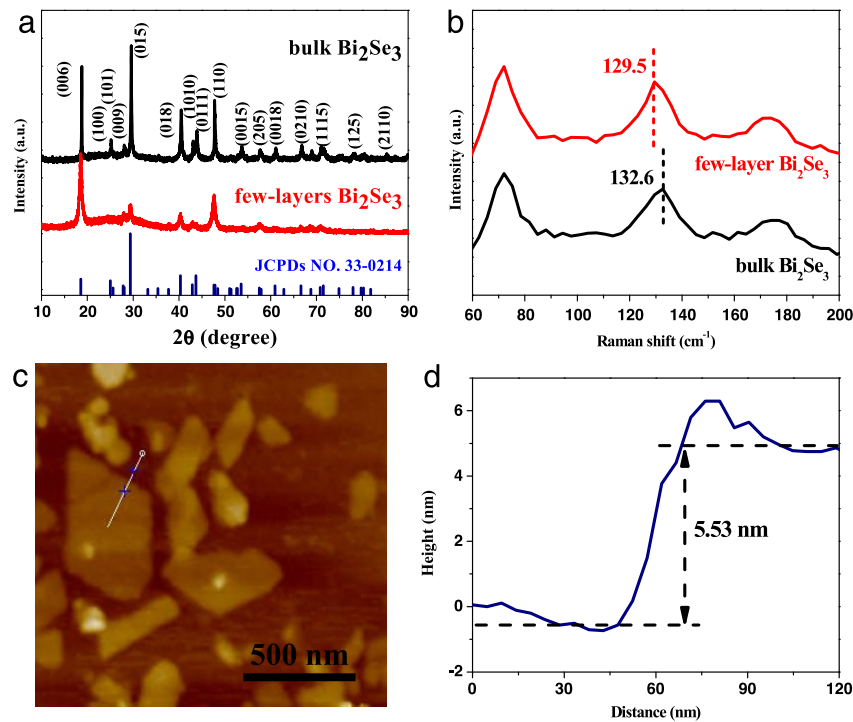


Fig. 1. (a) XRD and (b) Raman spectra of the bulk Bi_2Se_3 and few-layer Bi_2Se_3 samples; (c) AFM image and (d) height profile of an as-prepared few-layer Bi_2Se_3 sample.

medium, we have demonstrated Q-switched lasers not only at red (~ 640 nm) and orange ($\sim 607 + 604$ nm), but also at deep red (~ 721 nm).

2. Preparation and characterization of few-layer Bi_2Se_3 SA

The characterization of the newly prepared TI Bi_2Se_3 nanoplates is shown in Fig. 1. The bulk Bi_2Se_3 and the few-layer Bi_2Se_3 nanoplates are both characterized by X-ray diffraction (XRD) in Fig. 1(a). All the labeled peaks of the bulk Bi_2Se_3 can be easily indexed to rhombohedral Bi_2Se_3 (JCPDs NO. 33-0214). The few-layer Bi_2Se_3 nanoplates have been successfully exfoliated from bulk Bi_2Se_3 since the XRD pattern of the as-prepared Bi_2Se_3 nanoplates shows that some characteristic peaks disappeared. In Fig. 1(b), the characteristic peaks of bulk Bi_2Se_3 at 72.0 , 132.6 , and 173.9 cm^{-1} , are assigned to A_{1g}^1 , E_g^2 and A_{1g}^2 vibrational modes, respectively. The dashed lines in Fig. 1(b) indicate red shift of E_g^2 mode in few-layer Bi_2Se_3 from bulk Bi_2Se_3 . Furthermore, atomic force microscopy (AFM) image was used to characterize the thickness of the few-layer Bi_2Se_3 in Fig. 1(c). The as-prepared few-layer Bi_2Se_3 nanoplates were about 5.53 nm as the height profile shown in Fig. 1(d), which indicates the TI Bi_2Se_3 nanoplates are around 5 layers because the monolayer Bi_2Se_3 has been reported to be 0.96 nm in thickness measured with AFM.

The as-prepared few-layer Bi_2Se_3 solution was then transferred onto a 0.5 -mm-thin glass substrate by spin-coating method at low speed. We measured the transmission and absorption of the fabricated Bi_2Se_3 thin film with glass substrate from 400 nm to 1400 nm using PerkinElmer Lambda 750 spectrophotometer. Fig. 2 plots the measured transmission and absorption curves, in which for transmission a 92% transmission of the blank glass substrate was already subtracted. Thus, as can be seen, the final transmissions at 607 nm, 640 nm and 721 nm are 90.1% , 90.6% and 92.1% , respectively.

3. Experimental details

The schematic of laser experimental setup is shown in Fig. 3. The pump source is an InGaN blue LD with maximum output power of about 1.8 W and peak wavelength of 444 nm. A 75 -mm (focal length) lens with

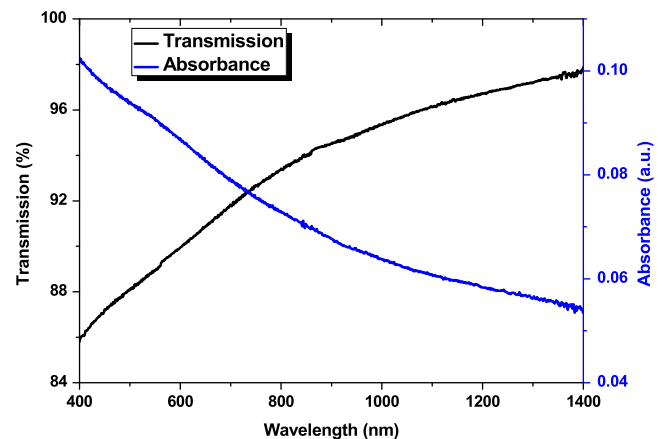


Fig. 2. Transmission and absorption measurements of the as-fabricated few-layer Bi_2Se_3 sample.

anti-reflection coating in blue was used to focus the pump beam into the laser crystal. Three two-mirror plane-concave cavities were individually used for the three lasers. Three flat mirrors, used for input mirrors (IMs), were coated with high transmission of about 90% at pump wavelength and high reflection of more than 99.8% at the three laser wavelengths. For 721 nm laser cavity, the IM has a transmission of 59.9% and 87.4% at 640 nm and 607 nm aiming at suppressing the two high-gain emission lines. For 607 nm laser cavity, the IM has a transmission of 36.2% at 640 nm. Three curved output couplers (OCs) were respectively used, all with curvature radii of 50 mm. The transmissions of three OCs are 4.1% for 640 nm, 3.3% for 721 nm and 2.7% for 607 nm.

The laser gain medium was a Pr:YLF crystal with cross section of 2×2 mm^2 and length of 8 mm in cavity-axis direction and dopant concentration of 0.2 at.%. In order to protect the laser crystal from thermal fracture, it was wrapped with indium foil and then mounted inside a 14 -mm-long copper block. The copper block was connected to a water-cooled chiller with setting temperature at 16 $^\circ\text{C}$. On the one

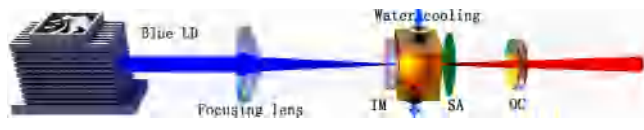


Fig. 3. Experimental setup photograph of diode-pumped Q-switched Pr:YLF visible lasers using Bi_2Se_3 as SA. IM: input mirror, OC: output coupler.

hand, the longer copper block can stop part of the residual pump beam and therefore can improve the output powers and stabilities of the lasers. On the other hand, the laser performances have also been paid special cares during the laser experiments by inserting Bi_2Se_3 SA at suitable distances between the laser crystal and OC. The physical lengths of the laser cavities for all laser operations were optimized to be about 46 mm during the laser experiments. The present laser cavity length was a little shorter than 50 mm, i.e. a length that is with respect to the so-called hemispherical cavity. Hemispherical cavity is probably easy to achieve laser generation because of its small cavity mode size and therefore low laser threshold. However, small mode size is not favorable to power scaling because of strong thermal effect inside the laser material and worse mode overlap between the pump beam and cavity mode. The present lengths of the laser cavities were determined by a simple fact that we have achieved maximum output powers with the lengths.

4. Results and discussion

After optimizing the continuous-wave laser cavities, Q-switching lasers at ~ 721 , ~ 640 and ~ 607 nm have been achieved by inserting the as-prepared Bi_2Se_3 SA. Q-switched laser operations at the three wavelengths were achieved with maximum output powers of 30.9 mW, 40.2 mW and 35.7 mW, as shown in Fig. 4. The slope efficiencies of the three wavelengths were fitted to be about 3.9%, 4.7% and 4.3%, respectively. In Fig. 4, the insets show the corresponding laser spectra of the three wavelengths in Q-switching modes. It should be pointed out that the 721 and 640 nm laser spectra show very similar spectral structure to the case of continuous-wave operation. However, for the single-wavelength 607 nm orange laser achieved in CW mode, there also existed a relatively weak 604 nm laser with peak of 604.36 nm (see inset in Fig. 4(c)) when operated at Q-switched mode. The lasing behavior was different from that reported in Ref. [16], but still with similarity. Instead of operating at 607 nm in CW mode, Ref. [16], demonstrated a pure 604 nm Q-switched laser by explaining reduced absorption loss with respect to the 604 nm line when the laser cavity was operated in Q-switched mode. The present laser behavior was probably due to the tilt angle of the glass substrate, which could also play a role as etalon. Further investigation, including on spectroscopy of Pr:YLF crystal specifically at the orange spectral region, should be carried out to present a conclusive explanation on the wavelength shift, which is now under investigation in our lab.

Fig. 5 shows the whole variations of pulse widths and pulse repetition rates with the increasing of absorbed powers for the Q-switched lasers at 721, 640 and 607/604 nm. As Fig. 5(a) shown, for the 721 nm laser, the pulse width narrowed steeply from 1116 ns to 368 ns till the absorbed power exceeding about 1500 mW. After that, the pulse width slightly broadened to 407 ns. During the whole period, the pulse repetition rate increased from 60.5 kHz to 185.2 kHz monotonously. For the 640 nm laser, the pulse width decreased from 963 ns to 210 ns with corresponding pulse repetition rate increased from 72.6 kHz to 263.1 kHz. For the 607 and 604 nm lasers, the pulse width decreased from 896 ns to 263 ns with corresponding pulse repetition rate increased from 78.6 kHz to 192.3 kHz.

Fig. 6 shows the oscilloscope traces of pulse trains at the highest repetition rates and of the narrowest pulse widths for these laser wavelengths, which were also mentioned above in Fig. 5. The pulse-to-pulse amplitude fluctuations of the Q-switched pulse trains were all

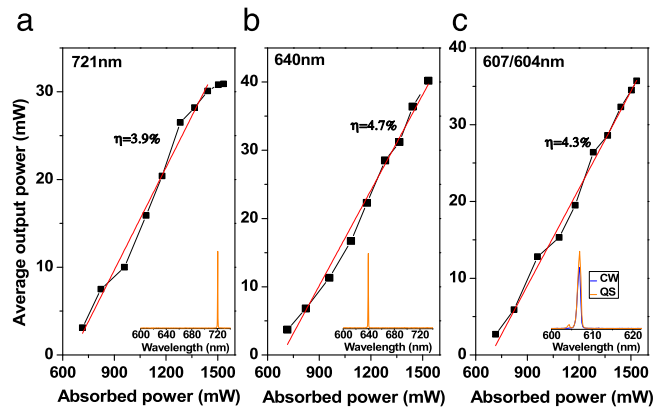


Fig. 4. Average output powers versus absorbed powers of (a) 721 nm, (b) 640 nm and (c) 607 and 604 nm lasers with corresponding laser spectra as insets.

measured to be less than about $\pm 8\%$. In addition, it should be pointed out that, in comparison to Ref. [16], the present shortest pulse widths of all the lasers that achieved in this work are far shorter. To explain the shorter pulse width, one of the reasons could be our shorter lengths of the laser cavities. In fact, according to Ref. [18], the pulse width is in proportion to the cavity round-trip time. As a consequence, our short laser cavity was of benefit to achieving short-pulse Q-switched laser.

Pursuing high pulse energy is in general an objective for Q-switched laser operation. We, according to these above data, can readily estimate the pulse energies of the laser emissions at different absorbed powers, which are shown in Fig. 7. In contrast to red 640 nm and orange 607/604 nm lasers, the pulse energy saturation of the deep red 721 nm laser was more obvious and emerged at lower absorbed power, which could be explained by the earlier saturation of its average output power and pulse width. From Fig. 7, one can find that the maximum pulse energies of the 721, 640 and 607/604 nm lasers to be about 0.17, 0.16 and 0.19 μJ , respectively. Correspondingly, we can also estimate the pulse peak power to be about 0.46, 0.73 and 0.71 W.

Finally, we compared the present results with that reported in other two publications, which also presented overall studies on the three visible lasers but using Pr:GLF crystal as gain medium, as well as two different nanomaterials as SAs, i.e. MoS_2 [9] and Au nanorods [10]. The results seem to be clear that the shortest pulse width achieved in this work is comparable to those two previous results. However, our pulse energies and peak powers are far better, which should be attributed to our higher average output powers.

5. Conclusion

In conclusion, using few-layer Bi_2Se_3 thin film as SA in this work, visible Q-switched laser operation at 721 nm and 640 nm, as well as simultaneous 607 nm and 604 nm have been demonstrated in a diode-pumped Pr:YLF crystal. The shortest pulse widths were achieved to be about 368 ns, 210 ns and 263 ns, respectively. Correspondingly, the maximum pulse energies and peak powers were about 0.17 μJ , 0.16 μJ and 0.19 μJ , as well as 0.46 W, 0.73 W and 0.71 W. The pulse width could be further narrowed by optimizing the laser cavity and by increasing the modulation depth of the Bi_2Se_3 SA. Thus, we hope that maximum pulse energy and peak power could reach μJ and W levels.

Acknowledgments

The authors wish to thank the financial support from National Natural Science Foundation of China (61275050), the Specialized Research Fund for the Doctoral Program of Higher Education (20130121120043) and Natural Science Foundation of Fujian Province of China (2014J01251).

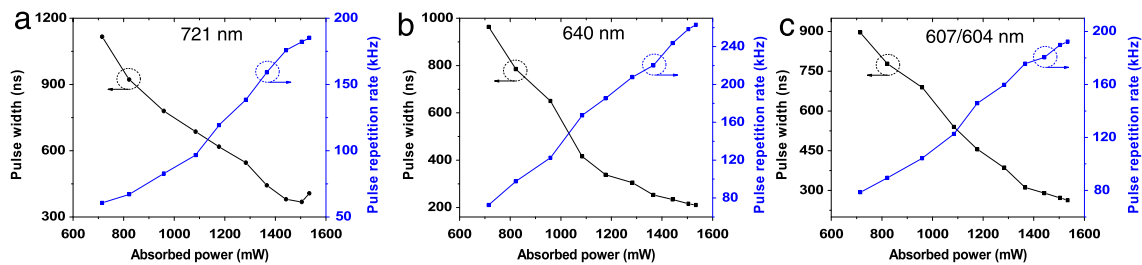


Fig. 5. The dependence of pulse width and repetition rate on absorbed power for (a) 721 nm, (b) 640 nm and (c) 607/604 nm lasers.

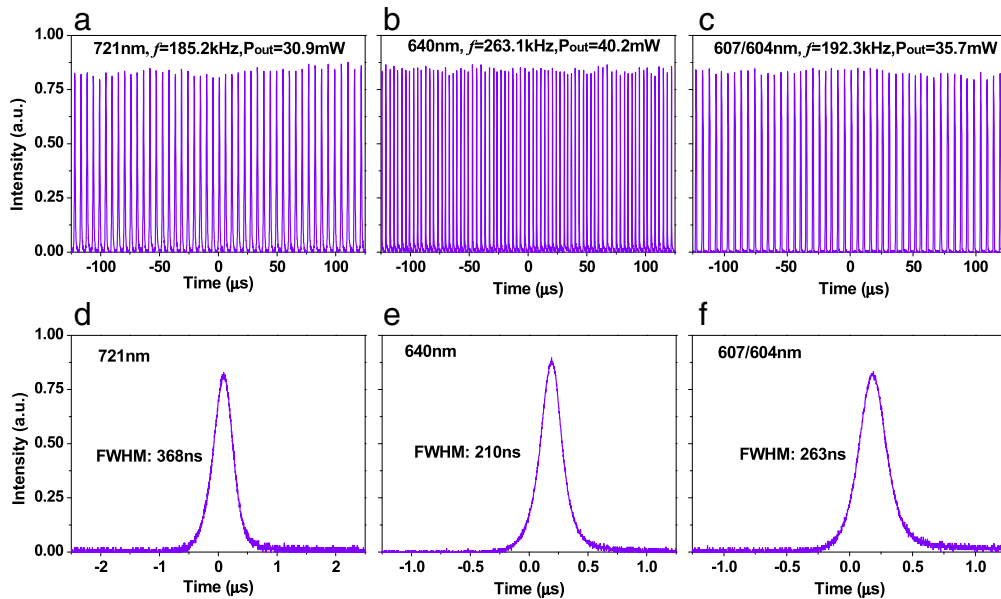


Fig. 6. Maximum pulse repetition rate and the shortest single pulse time duration of (a,d) 721 nm, (b,e) 640 nm and (c,f) 607/604 nm lasers.

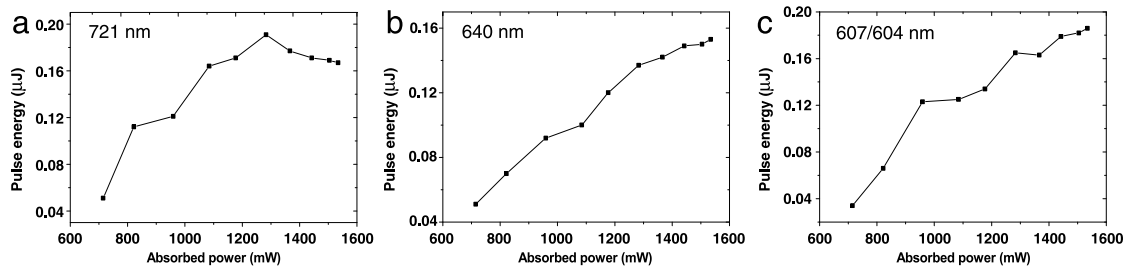


Fig. 7. Pulse energies varying from the absorbed powers for the Q-switched lasers at (a) 721 nm, (b) 640 nm and (c) 607/604 nm.

References

- [1] H. Zhang, Q.L. Bao, D.Y. Tang, L.M. Zhao, K.P. Loh, Large energy soliton erbium-doped fiber laser with a graphene-polymer composite mode locker, *Appl. Phys. Lett.* 95 (2009) 141103.
- [2] Z.Q. Luo, Y.Z. Huang, M. Zhong, Y.Y. Li, J.Y. Wu, B. Xu, H.Y. Xu, Z.P. Cai, J. Peng, J. Weng, 1-, 15-, and 2- μm fiber lasers Q-switched by a broadband few-layer MoS_2 saturable absorber, *IEEE J. Lightwave Technol.* 32 (24) (2014) 4077.
- [3] C.J. Zhao, H. Zhang, X. Qi, Y. Chen, Z.T. Wang, S.C. Wen, D.Y. Tang, Ultra-short pulse generation by a topological insulator based saturable absorber, *Appl. Phys. Lett.* 101 (2012) 211106.
- [4] R. Zhang, Y.X. Zhang, H.H. Yu, H.J. Zhang, R.L. Yang, B.C. Yang, Z.Y. Liu, J.Y. Wang, Broadband black phosphorus optical modulator in the spectral range from visible to mid-infrared, *Adv. Funct. Mater.* 3 (2015) 1787–1792.
- [5] B. Xu, Y.J. Cheng, Y. Wang, Y.Z. Huang, J. Peng, Z.Q. Luo, H.Y. Xu, Z.P. Cai, J. Weng, R. Moncorgé, Passively Q-switched Nd:YAlO_3 nanosecond laser using MoS_2 as saturable absorber, *Opt. Express* 22 (23) (2014) 28934–28940.
- [6] J.J. Liu, J. Liu, Z.N. Guo, H. Zhang, W.W. Ma, J.Y. Wang, L.B. Su, Dual-wavelength Q-switched Er:SrF_2 laser with a black phosphorus absorber in the mid-infrared region, *Opt. Express* 24 (26) (2016) 30289–30295.
- [7] C. Li, J. Liu, S.Z. Jiang, S.C. Xu, W.W. Ma, J.Y. Wang, X.D. Xu, L.B. Su, 28 μm passively Q-switched Er:CaF_2 diode-pumped laser, *Opt. Mater. Express* 6 (5) (2016) 1570–1575.
- [8] M.Q. Fan, T. Li, S.Z. Zhao, G.Q. Li, H.Y. Ma, X.C. Gao, C. Krankel, G. Huber, Watt-level passively Q-switched $\text{Er:Lu}_2\text{O}_3$ laser at 2.84 μm using MoS_2 , *Optim. Lett.* 41 (3) (2016) 540–543.
- [9] Y. Zhang, S. Wang, H. Yu, H. Zhang, Y. Chen, L. Mei, A.D. Lieto, M. Tonelli, J. Wang, Atomic-layer molybdenum sulfide optical modulator for visible coherent light, *Sci. Rep.* 5 (2015) 11342.
- [10] S. Wang, Y. Zhang, J. Xing, X. Liu, H. Yu, A.D. Lieto, M. Tonelli, T. ChienSum, H. Zhang, Q. Xiong, Nonlinear optical response of Au nanorods for broadband pulse modulation in bulk visible lasers, *Appl. Phys. Lett.* 107 (2015) 161103.
- [11] Ryo Abe, Junichiro Kojou, Kensuke Masuda, Fumihiko Kannari, Cr^{4+} -doped $\text{Y}_3\text{Al}_5\text{O}_{12}$ as a saturable absorber for a Q-switched and mode-locked 639-nm Pr^{3+} -doped LiYF_4 laser, *Appl. Phys. Express* 6 (2013) 032703.

- [12] H.H. Yu, H. Zhang, Y.C. Wang, C.J. Zhao, B.L. Wang, S.C. Wen, H.J. Zhang, J.Y. Wang, Topological insulator as an optical modulator for pulsed solid-state lasers, *Laser Photon. Rev.* 7 (6) (2013) L77–L83.
- [13] Z.Q. Luo, Y.Z. Huang, J. Weng, H. Cheng, Z.Q. Lin, B. Xu, Z.P. Cai, H.Y. Xu, 106 μm Q-switched ytterbium-doped fiber laser using few-layer topological insulator Bi_2Se_3 as a saturable absorber, *Opt. Express* 21 (24) (2013) 29516.
- [14] B. Xu, Y. Wang, J. Peng, Z.Q. Luo, H.Y. Xu, Z.P. Cai, J. Weng, Topological insulator Bi_2Se_3 based Q-switched $\text{Nd}:\text{LiYF}_4$ nanosecond laser at 1313 nm, *Opt. Express* 23 (6) (2015) 7674.
- [15] D. Wu, Z.P. Cai, Y. Zhong, J. Peng, J. Weng, Z.Q. Luo, N. Chen, H.Y. Xu, 635-nm Visible Pr^{3+} -doped ZBLAN fiber lasers Q-switched by topological insulators SAs, *Photon. Technol. Lett.* 27 (22) (2015) 2379.
- [16] Y.J. Cheng, J. Peng, B. Xu, H.Y. Xu, Z.P. Cai, J. Weng, Passive Q-switching of $\text{Pr}:\text{LiYF}_4$ orange laser at 604 nm using topological insulators Bi_2Se_3 as saturable absorber, *Opt. & Laser Technol.* 88 (2017) 275–279.
- [17] P.H. Tang, M. Wu, Q.K. Wang, L.L. Miao, B. Huang, J. Liu, C.J. Zhao, S.C. Wen, 28- μm pulsed $\text{Er}^{3+}:\text{ZBLAN}$ fiber laser modulated by topological insulator, *Photon. Technol. Lett.* 28 (14) (2016) 1573–1576.
- [18] G.J. Spuhler, R. Paschotta, R. Fluck, B. Braun, M. Moser, G. Zhang, E. Gini, U. Keller, Experimentally confirmed design guidelines for passively Q-switched microchip lasers using semiconductor saturable absorbers, *J. Opt. Soc. Amer. B* 16 (3) (1999) 376–388.